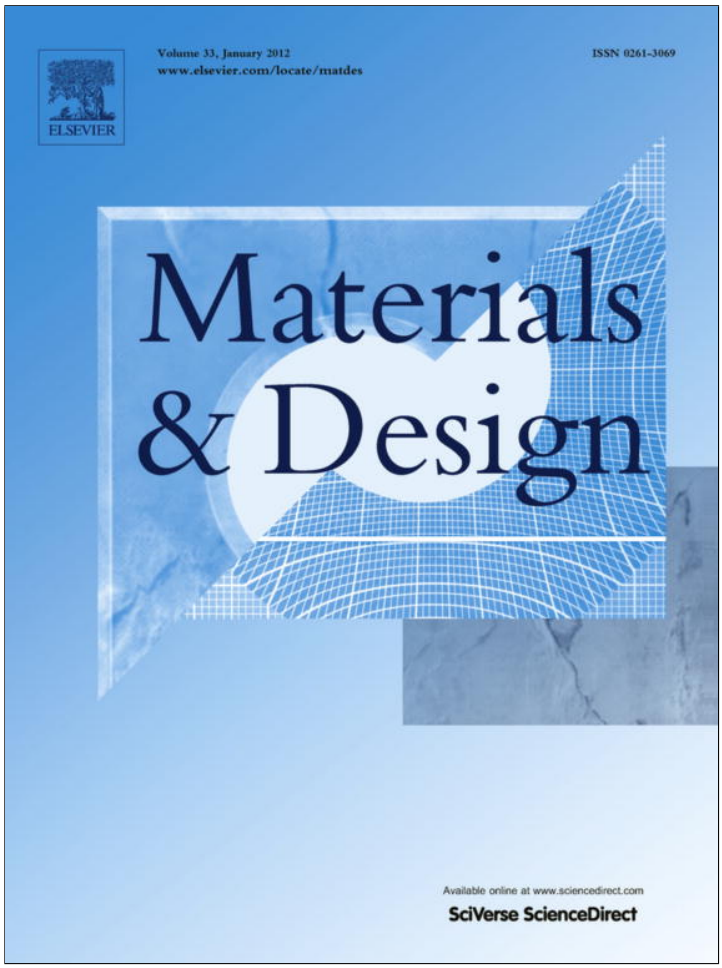

(This is a sample cover image for this issue. The actual cover is not yet available at this time.)

Materials and Design 41 (2012) 421–432

Contents lists available at SciVerse ScienceDirect

Materials and Design

journal homepage: www.elsevier.com/locate/matdes

Brittle fracture of U-notched graphite plates under mixed mode loading

F. Berto, P. Lazzarin *, C. Marangon

University of Padova, Department of Management and Engineering, Stradella S. Nicola 3, 36100 Vicenza, Italy

ARTICLE INFO

Article history:
Received 12 March 2012
Accepted 10 May 2012
Available online 18 May 2012

Keywords:
Mixed mode
Brittle failure
Elasticity
Blunt notches

ABSTRACT

Brittle fracture of isostatic polycrystalline graphite is studied experimentally, theoretically and numerically using U-notched samples under mode I and mixed mode loading (I + II) considering different combinations of the notch radius and the tilt angle of the notch. An experimental programme was performed to provide a new set of results. In total 60 new data are provided in the paper.

The averaged value of the strain energy density over a control volume is used to assess the static strength of the specimens subjected to different mode mixities. The volume is centred where the principal stress reaches its maximum value on the notch edge, by rigidly rotating the crescent-shaped volume already used in the literature to analyse U- and V-shaped notches subject to mode I loading. The volume size depends on the fracture toughness and the ultimate tensile strength of the material. Good agreement is found between experimental data and theoretical predictions based on the constancy of the mean strain energy density over the control volume.

1. Introduction

Several criteria have been proposed for the failure assessment of brittle or quasi-brittle materials under monotonic loading subjected to mode I and weakened by sharp and blunt notches.

A "Line criterion" was applied by Knésl who dealt with components weakened by sharp V-shaped notches [1]. Some important aspects of the stress field in the proximity of the notch tip were highlighted by Nui et al. who demonstrated that, for distances from the notch tip less than 0.2 times the notch radius, stress distributions along the notch bisector depend only on the notch root and not on the opening angle [2]. Seweryn provided a set of experimental data from sharp V-notches specimens made of PMMA and applied a criterion where the asymptotic stresses governed by the notch stress intensity factor (NSIF) were integrated over a material-dependent distance from the point of singularity [3]. Strandberg successfully applied the NSIF criterion to V-notched samples made of annealed tool steel, AISI O1, tested at −50 °C [4]. Dealing with different ceramic materials, Gogotsi investigated the sensitivity of the mode I fracture toughness as a function of the notch tip radius [5].

Considering failures from sharp and blunt notched specimens the Cohesive Zone Model (CZM) criterion has been successfully used and continuously improved considering the influence of different softening curve for the material [6,7]. Two essential parameters are associated with the softening curve: the ultimate tensile strength σ_t and the specific fracture energy G_f. Just considering linear elastic behaviour and ideally sharp notches, Gómez and Elices [7] were able to demonstrate that a single non-dimensional curve fits the experimental data from V-notched specimens made of steel, aluminium, polymethyl-metacrylate (PMMA) and PVC.

In a recent contribution [8], by using the Ansys code, the cohesive zone model, which is known as a variation in the cohesive stresses with the interfacial opening displacement along the localised fracture process zone, has been applied by Ghasemnejad and Aboutorabi to assess the mode I and mode II delamination failure in laminated composite structures.

In parallel a criterion based on the strain energy density (SED) averaged over a control volume was developed in Refs. [9,10] for static and fatigue strength assessments of notched components and welded joints. By using the SED approach, Yosibash et al. showed a very good correlation to a large amount of experimental data from Alumina–7% Zirconia and PMMA specimens [11]. A criterion based on the *J*-integral has been proposed by Matvienko and Morozov for a body with a U-notch considering an elastic and elastic–plastic behaviour of the material [12]. The *J*-integral has been recently applied to homogeneous plates and functionally graded aluminium–silicone carbide composite with U-notches under bending loading [13,14]. A modified maximum tangential stress criterion has been proposed for fracture assessment of plates weakened by blunt V-notches [15]. An accurate review of the main criteria applicable under prevalent mode I loading is carried out in Ref. [16].

Under mixed mode loading, particularly for notches with a non-negligible radius, providing a suitable fracture criterion is more complex than under mode I loading because the maximum

* Corresponding author. Tel.: +39 0444998780; fax: +39 0444998888.
E-mail address: plazzarin@gest.unipd.it (P. Lazzarin).

0261-3069/$ - see front matter © 2012 Elsevier Ltd. All rights reserved.
http://dx.doi.org/10.1016/j.matdes.2012.05.022

elastic stress is out of the notch bisector line and its position varies as a function of mode I to mode II stress distributions, along the notch edge. For this reason, the problem of brittle or quasi-brittle fracture of blunt notched components loaded under mixed mode (I + II) requires further investigations. Another important reason is the scarcity of experimental results available in the literature, in particular dealing with blunt notches under prevalent mode II loading and, then, the possibility to set up an approach for the fracture assessment under the above mentioned conditions.

The proposal of mode I dominance for crack plates was suggested first by Erdogan and Sih when dealing with cracked plates under plane loading and transverse shear, where the crack grows in the direction almost perpendicular to the maximum tangential stress in radial direction from its tip [17]. Dealing with the strain energy density concept, it is worthwhile contemplating some fundamental contributions provided by Sih [18]. The strain energy density factor S [18] was defined as the product of the strain energy density by a critical distance from the point of singularity. Failure was thought of as controlled by a critical value S_c, whereas the direction of crack propagation was determined by imposing a minimum condition on S. Several criteria have been applied mainly to sharp V-notched samples but also to U-notches [19–25] showing a different degree of accuracy with respect to the experimental results. Seweryn and Lucaszewicz reviewed the main criteria available under mixed mode loading [20]. A failure criterion at re-entrant corners in brittle elastic materials, validated in [11] for mode I loading, was extended to mixed mode loading and validated by experimental observations [21,22]. Chen and Ozaki provided some interesting results under mixed mode loading. However, the prevalent mode during the test was mode I [23]. A modified maximum tangential stress criterion has been developed to predict the fracture toughness and fracture initiation angle in U-shaped notches under mixed mode loading or prevalent mode II loading [24,25].

In the latest years a criterion based on the strain energy density (SED) over a control volume has been developed [9,10,26] and applied to assess failure from cracked, U-notched and sharp V-notched components and also from structural components [27,28]. Over a small but finite volume of material close to the notch, the energy always has a finite value. Lazzarin and Zambardi [9] predicted the static and fatigue behaviour of components weakened by sharp V-notches with variable notch angles using the mean value of the local strain energy. The control radius R_c of the volume, over which the energy was averaged, depended on the fracture toughness and the ultimate tensile stress in the case of static loads and brittle materials. Different from Sih's criterion, which is a point-wise criterion, the averaged strain energy density criterion (SED) states that brittle failure occurs when the mean value of the strain energy density over a control volume (which becomes an area in two dimensional cases) is equal to a critical energy W_c.

The SED criterion has been recently extended to mixed mode loading (see Refs. [29–34]).

The equivalent local mode I concept on U-notched specimens has been applied by moving the control volume along the notch edge in such a way that it is centred in relation to the maximum elastic stress [29–31] and a simply but accurate expression has been found to evaluate the SED once the maximum value of the principal stress along the notch edge is known [30,34]. The SED criterion has been widely compared with the CZM in Ref. [30].

This criterion is used in the present contribution to assess the brittle fracture on graphite U-notched specimens. Isostatic graphite is manufactured by using cold isostatic pressing technique and is often known for its homogeneous structure and excellent isotropic electrical, thermal properties. Moreover this kind of graphite is known for its high mechanical performances and for this reason is used in mechanical applications. It is sometimes purified in special-designed graphitization furnace to remove non-carbonaceous inclusions and impurities. Isostatic graphite is extensively used in various industrial applications such as: moulds in continuous casting systems for making shaped steel, cast iron and copper; crucibles for melting precious metals or alloys; moulds for making shaped glass; heating elements, heat shields, crucibles, etc.

There are various practical conditions where the notches in graphite components are subjected to a combination of tensile and shear deformation (or mixed mode I/II loading). Cracks on graphite components are generated by manufacturing faults and other defects are also due to the coalescence of the micro-structural pores that are inherently embedded in graphite. While cracks are viewed as unpleasant entities in most engineering materials, notches of U or V-shape are sometimes desirable in design and manufacturing of products made from graphite. Moulds, heating elements and chucks are only some examples of industrial graphite components that contain U or V-shape notches.

Extensive studies on mode I and mixed mode fracture in cracked graphite specimens are present in literature but very few papers have dealt with brittle fracture in V-shaped and U-shaped notched graphite components. Ayatollahi and Torabi [35] conducted a series of fracture tests on three different V-notched test specimens made of a polycrystalline graphite material. Instead Ayatollahi et al. [36] recently performed some tests on brazilian disk specimens to investigate failures on polycrystalline graphite weakened by blunt V-notches. Some tests have been recently carried out also considering graphite bars weakened by V-notches subjected to torsion loading [37].

Finally, worth mentioning are the modelling efforts to predict the influence of microstructure on damage tolerance of a polygranular nuclear graphite documented by Mostafavi and Marrow in [38], based on direct observation of crack nucleation and growth. The digital image correlation was used to measure the full field displacements on the surface of large specimens as well as for early detection and characterisation of fracture nuclei (short cracks) under repeated cyclic loadings [38].

The present research deals with mixed mode (I + II) brittle fracture of U-notched specimens made of isostatic graphite.

The purpose of the present research is twofold:

a. To provide a large body of experimental data from static fracture of notched graphite specimens subjected to mixed mode loading with varying notch root radii and different mode mixities. Such data should be helpful to engineers engaged in static strength analysis of graphite components. Sixty new experimental results are summarised in the paper with reference to various notch configurations.
b. To provide a fracture model in order to estimate the critical loads to failure in notched isostatic graphite components subjected to in plane mixed mode loading. The strain energy density averaged on a control volume is used for brittle failure assessments of notched graphite samples in mixed mode I/II loading conditions.

The paper is structured in the following way: in the first section the experimental work is described including specimen geometries, testing procedures and experimental results. The second section is focused on the SED criterion applied to U-notches and to the numerical models. Finally, the third section presents a synthesis of all data in terms of averaged SED using a control volume based on the basic material properties under mixed mode loading and a final discussion of the present results.

2. Fracture experiments

2.1. Materials and geometry

The material used is a commercial isostatic graphite particularly used in mechanical applications for its high performances. The mean grain size was measured by using the SEM technique and the density was determined from the buoyancy method.

Table 1 presents the most important material properties: mean grain size is 2 μm, porosity 7%, bulk density of 1850 kg/m^3, tensile strength of 46 MPa, Young's modulus of 8.05 GPa and shear modulus 3.35 GPa. The flexural strength is 49 MPa, whereas the compressive strength is equal to 110 MPa. In a previous investigation [36], the detected mean grain size was 320 μm whereas the tensile strength was equal to 27.5 MPa, resulting in a mechanical behaviour very different from that of the isostatic graphite considered in the present work. A mean strength of 27.9 MPa characterised also the poly-granular nuclear graphite investigated in Ref. [38].

All tests were performed under load control on a servocontrolled MTS axial testing device (±100 kN/±110 Nm, ±75 mm/±55°). The load was measured by a MTS cell with ±0.5% error at full scale.

The samples used in this investigation are plates with a central blunt U-notch, as shown in Fig. 1. Different radii at the notch tip, ρ, and tilt angles of the notch, β, are used in order to investigate their influence on the failure. All the specimens are subjected to tensile load. By varying the tilt angle β different mode-mixity can be produced. If the tilt angle is equal to zero the notches are subjected to pure mode I, while varying β the loading condition changes from pure mode I towards mixed mode I + II. For all the tested graphite specimens, the width, the distance between the tip of the notches and the thickness were 50 mm, 10 mm and 10 mm, respectively.

Five values of notch radius ρ = 0.25, 0.5, 1, 2, 4 mm were considered for manufacturing the test specimens so that the effects of the notch tip radius on mixed mode fracture of the graphite specimens are studied. With the aim to obtain different mode mixities four values of the angle β were considered ($\beta = 0°$, $\beta = 30°$, $\beta = 45°$ and $\beta = 60°$). Figs. 2 and 3 show some photos of the tested specimens and some details of the notches.

2.2. Experimental procedure

In order to prepare the graphite test specimens (see Figs. 2 and 3), first several plates of 10 mm thick were cut from a graphite block. Then, the specimens were precisely fabricated by using a 2-D CNC water-jet cutting machine. The thickness of the specimens was chosen following the guidelines drawn in Refs. [39,40] with the aim to assure plane strain conditions at the notch tip.

Before conducting the experiments, the cut surfaces of the graphite specimens were polished by using a fine abrasive paper to remove any possible local stress concentrations due to surface roughness. A total number of 60 mixed mode I/II fracture tests were performed for various notch geometry parameters. For each geometry shape and loading angle, three separate fracture tests were performed by using a universal tension–compression test machine under displacement-control conditions with a loading rate of 0.05 mm/min. The load–displacement curves recorded during the fracture tests were all linear and the specimens fractured suddenly. Therefore, the use of a brittle fracture criterion based on the linear elastic fracture mechanics (LEFMs) is permissible. The values of the fracture loads for each experimental test and the mean values ($\langle F \rangle$) recorded by the test machine are presented in Table 2.

Table 1
Mechanical properties.

Material property	Value
Elastic modulus, E (MPa)	8050
Shear modulus, G (MPa)	3354
Poisson's ratio, ν	0.2
Ultimate torsion strength (MPa)	30
Ultimate compression strength (MPa)	110
Ultimate tensile strength (MPa)	46
Fracture toughness (MPa m$^{0.5}$)	1.06
Density (kg/dm^3)	1.85
Porosity (%)	7
Resistivity (μohm m)	11
Thermal conductivity (W/(m K))	110

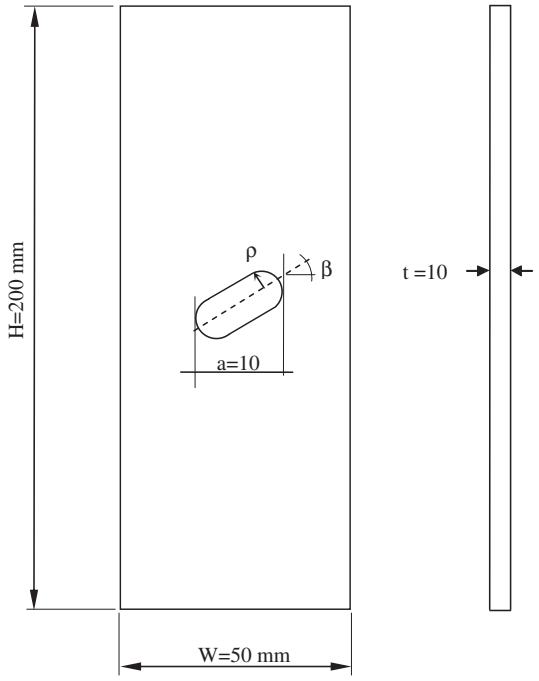

Fig. 1. Geometry and main dimensions of the tested specimens.

A re-analysis of Table 2 shows that the fracture load increases when the radius ρ increases from 0.25 mm to 4 mm.

Dealing with crack initiation angles they have been measured experimentally by using an optical microscope and a dedicate software called Las (Leica Application Suite), see Fig. 4 as example. All the values of the initial crack angles are reported in Table 2 also with the mean value of the three performed tests ($\langle \varphi \rangle$).

2.3. Mode mixity

In order to quantify the mode mixity of the tested specimens, some FE analyses were carried out. In agreement with Ref. [41] the definition of generalised notch stress intensity factors (N-SIFs) for mode I and mode II is as follows:

$$K_{I\rho} = \sqrt{2\pi r}\frac{(\sigma_\theta)_{\theta=0}}{1+\frac{\rho}{2r}}$$
$$K_{II\rho} = \sqrt{2\pi r}\frac{(\tau_{r\theta})_{\theta=0}}{1-\frac{\rho}{2r}} \quad (1)$$

where σ_θ and $\tau_{r\theta}$ are the stresses along the notch bisector line at a distance r from the local frame origin placed at a distance $\rho/2$ from the notch tip.Eq. (1) is not expected to give a constant value for N-SIFs but slight variations are possible. The slightly oscillating trend ahead of the notch tip is widely investigated in Refs. [41,42]. In or-

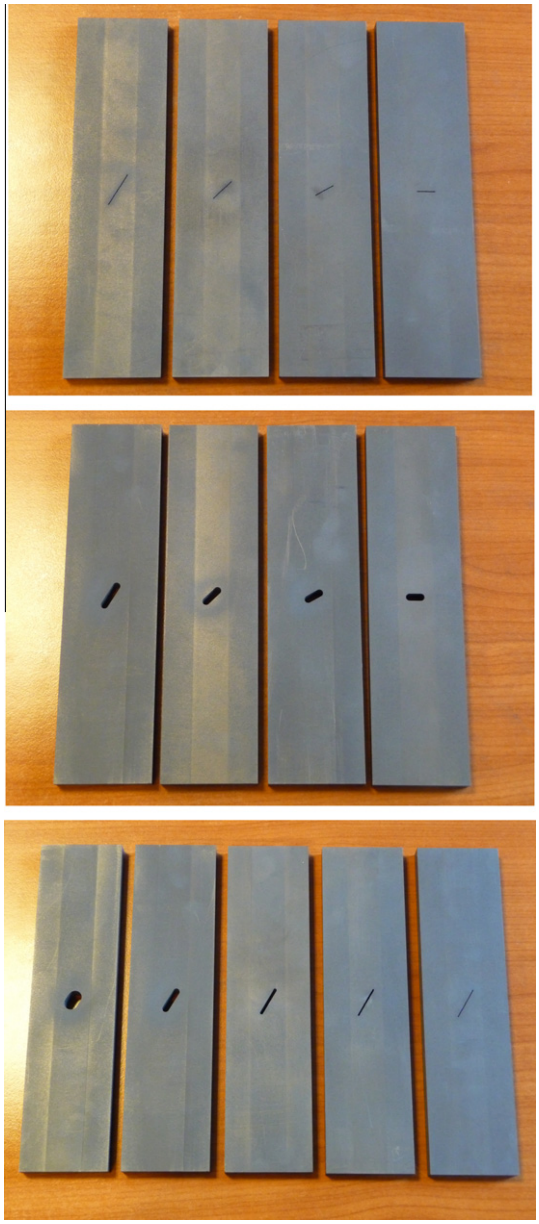

Fig. 2. Different U-notched specimens: (a) $\rho = 0.25$ (b) $\rho = 2$ mm (c) $\beta = 60°$.

der to eliminate the weak dependence on the notch tip distance, the following expressions have been defined to calculate the mean values of the generalised NSIFs [41]:

$$\overline{K}_{1\rho} = \frac{1}{\eta\rho}\int_{\rho/2}^{\rho/2+\eta\rho}(K_{1\rho})dr$$
$$\overline{K}_{\rho,\mathrm{II}} = \frac{1}{\eta\rho}\int_{\rho/2}^{\rho/2+\eta\rho}(K_{\mathrm{II}\rho})dr \quad (2)$$

where η is set equal to 0.2 in the present paper.

The mode mixity has been defined according to the following definition

$$\chi = \frac{2}{\pi}\arctan\left[\frac{\overline{K}_{\mathrm{II}\rho}}{\overline{K}_{1\rho}}\right] \quad (3)$$

The values of χ are listed in Table 3 and varies from 0 (pure mode I) to 0.9 (prevalent mode II).

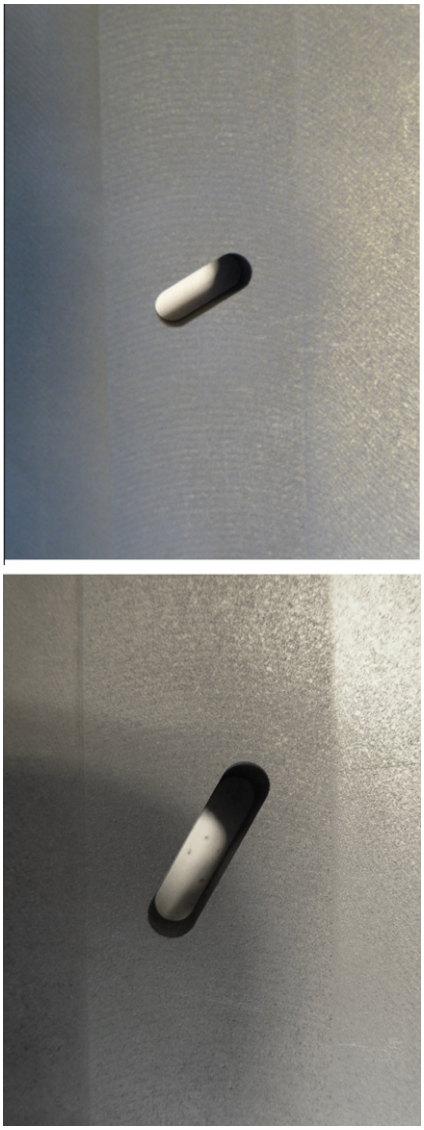

Fig. 3. Views of two different inclined U-notches: (a) $\rho = 2$ mm, $\beta = 30°$ (b) $\rho = 2$ mm, $\beta = 60°$.

Dealing with mode II notch stress intensity factors some recent developments can be found in Ref. [42]. In particular by taking advantage of some analytical formulations which are able to describe stress distributions ahead of parabolic, hyperbolic and V-shaped notches with end holes, the paper discusses the form and the significance of the NSIFs with reference to in-plane shear loading, considering explicitly the role played by the notch opening angle and the notch tip radius.

3. SED criterion applied to U-notches and numerical models

The averaged strain energy density criterion (SED) as presented in Ref. [9] states that brittle failure occurs when the mean value of the strain energy density over a given control volume is equal to a critical value W_c. This critical value varies from material to material but does not depend on the notch geometry and sharpness. The control volume is thought of as dependent on the ultimate tensile strength and the fracture toughness K_{Ic} in the case of brittle or quasi-brittle materials subjected to static loads. For a blunt U-notch under mode I loading, the volume assumes the crescent shape shown in Fig. 5a, where R_c is the depth measured along the notch bisector line. The outer radius of the crescent shape is equal to R_c

Table 2
Experimental critical loads and initial crack angles.

β (°)	ρ (mm)	F_1 (N)	F_2 (N)	F_3 (N)	$\langle F \rangle$ (N)	φ_1	φ_2 (°)	φ_3	$\langle \varphi \rangle$ (°)
		Exp.				Exp.			
0	0.25	4115	4708	4455	4426	0	0	0	0
	0.5	4592	4495	4429	4505	0	0	0	0
	1	4461	5152	4830	4814	0	0	0	0
	2	5182	5824	5541	5516	0	0	0	0
	4	7083	6406	6879	6789	0	0	0	0
30	0.25	3979	4009	4114	4034	35.82	28.78	27.87	30.82
	0.5	4254	4422	4370	4349	28.60	43.10	34.79	35.50
	1	4756	4829	4888	4824	32.95	29.26	28.13	30.11
	2	5906	5965	5876	5916	26.05	29.53	29.31	28.30
	4	6685	7098	6875	6886	27.68	33.06	30.74	30.49
45	0.25	3848	3954	3979	3927	53.99	33.26	40.10	42.45
	0.5	4302	4164	4318	4261	46.55	48.00	44.62	46.39
	1	4756	4846	4729	4777	44.81	52.52	50.54	49.29
	2	5448	5666	5696	5603	47.94	42.61	41.91	44.15
	4	7041	6799	6747	6862	43.67	49.79	50.06	47.84
60	0.25	4034	3847	3944	3942	65.01	51.54	58.15	58.23
	0.5	4536	4491	4626	4551	64.97	48.84	53.70	55.84
	1	4697	4829	4810	4779	64.21	58.06	59.95	60.74
	2	5511	5363	5491	5455	59.79	54.21	55.72	56.57
	4	6941	6602	6704	6749	59.49	55.94	58.94	58.12

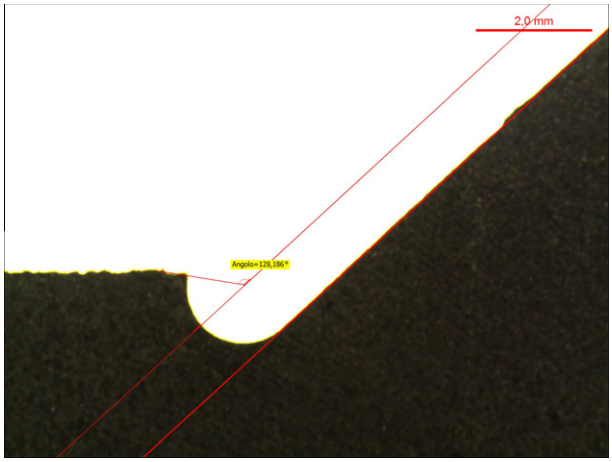

Fig. 4. Experimental measure of the initial crack angle with the dedicated software LAS.

Table 3
Mode mixity of the investigated geometries.

β (°)	ρ (mm)	$\overline{K}_{I\rho}/\sigma_{nom}$ (mm$^{0.5}$)	$\overline{K}_{II\rho}/\sigma_{nom}$ (mm$^{0.5}$)	$\overline{K}_{II\rho}/\overline{K}_{I\rho}$	χ
0	0.25	4.63	0.00	0.00	0.00
0	0.5	4.78	0.00	0.00	0.00
0	1	4.99	0.00	0.00	0.00
0	2	5.31	0.00	0.00	0.00
0	4	5.81	0.00	0.00	0.00
30	0.25	3.71	3.81	1.03	0.51
30	0.5	3.78	4.10	1.08	0.53
30	1	3.89	4.58	1.18	0.55
30	2	4.05	5.41	1.33	0.59
30	4	4.30	6.85	1.60	0.64
45	0.25	2.71	4.89	1.80	0.68
45	0.5	2.72	5.22	1.92	0.69
45	1	2.73	5.76	2.12	0.72
45	2	2.73	6.71	2.46	0.75
45	4	2.71	8.35	3.08	0.80
60	0.25	1.60	5.18	3.23	0.81
60	0.5	1.54	5.47	3.56	0.83
60	1	1.44	5.94	4.13	0.85
60	2	1.27	6.77	5.31	0.88
60	4	0.97	8.17	8.44	0.92

$+ \rho/2$, being $\rho/2$ the distance between the notch tip and the origin of the local coordinate system.

Under mixed mode loading the critical volume is no longer centred on the notch tip, but rather on the point where the principal stress reaches its maximum value along the edge of the notch (Fig. 5b). It was assumed that the crescent shape volume rotates rigidly under mixed mode, with no change in shape and size. This is the governing idea of the '*equivalent local mode I*' approach, as proposed and applied to U-notches [29,30].

Some closed-form expressions correlating SED and maximum elastic stress are reported in the literature [30]. In this paper, however, to avoid any simplified assumption, the SED values will be those directly determined from FE models.

Under plane strain conditions the critical length, R_c, can be evaluated according to the following expression [11,26]:

$$R_C = \frac{(1+\nu)(5-8\nu)}{4\pi}\left(\frac{K_{Ic}}{\sigma_t}\right)^2 \tag{4}$$

where K_{Ic} is the fracture toughness, ν the Poisson's ratio and σ_t the ultimate tensile stress of a plain specimen that obeys a linear elastic behaviour.

This critical value can be determined from the ultimate tensile stress σ_t according to Beltrami's expression:

$$W_c = \frac{\sigma_t^2}{2E} \tag{5}$$

Unnotched specimens often exhibit a non-linear behaviour whereas the behaviour of notched specimens remains linear. Under these circumstances the stress σ_t should be substituted by the maximum normal stress existing at the edge at the moment preceding the cracking, as underlined in Ref. [3] where it is also recommended to use tensile specimens with large semicircular notches to avoid any notch sensitivity effect.

In parallel, the control volume definition *via* the control radius R_c needs the knowledge of the fracture toughness K_{Ic} and the Poisson's ratio ν, see Eq. (4). The critical load that is sustainable by a notched component can be estimated by imposing $\overline{W}$ equal to the critical value W_c. This value is considered here constant under mode I, mode II and in plane mixed-mode conditions. This assumption has been extensively verified for a number of different brittle

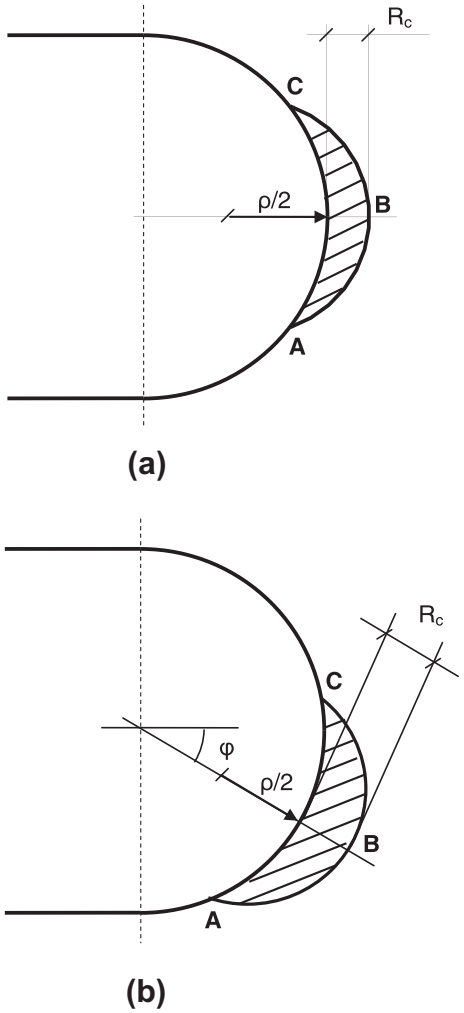

Fig. 5. Control volume under mode I (a) and mixed mode loading (b) for U-notched specimens.

and quasi-brittle materials [29,30]. Dealing with blunt notches under mixed mode loading, the problem becomes more complex than under mode I loading, mainly because the maximum elastic stress is out of the notch bisector line and its position varies as a function of mode I and mode II.

As discussed above, the idea of the '*equivalent local mode I*' approach, as proposed and applied to plates made of PMMA and weakened by U-notches [29,30], is used here. The critical volume is no longer centred on the notch tip, but rather on the point where the principal stress reaches its maximum value along the edge of the notch and it is assumed that the crescent shape volume rotates rigidly under mixed mode, with no change in shape and size with respect to mode I.

The maximum stress occurring along the edges of V-notches has been calculated numerically by using the FE code ANSYS 12.0®. For each geometry, two models were created. The first model was mainly oriented to the determination of the point where the maximum principal stress and the maximum SED were located; the second model was more refined, with an accurate definition of the control volume where the strain energy density should be averaged. All the analyses have been carried out by using eight-node elements under the hypothesis of plane strain conditions (see Fig. 6). The procedure for building the two models necessary to determine the SED in the rotated volume can be easily automated by simply writing an APDL (ANSYS Parametric Design Language) subroutine which permits the direct evaluation of the SED in the control volume.

Fig. 7 shows the shape of the control volume in the case of $\beta = 45°$, with $\rho = 0.25$ mm (a and b) and $\rho = 2$ mm (c and d). The contour lines of the maximum principal stress (a and c) as well as the SED isolines (b and d) are shown in the figure. As discussed in Ref. [26], the volume adapts itself varying the notch tip radius ρ.

Fig. 7 shows that a relatively refined mesh was used to model the notch profiles. However, one of the most important advantages of the SED approach is that to provide a mean value which is substantially mesh independent. In fact, contrary to some stress parameters integrated in the local criteria (e.g. maximum principal stress, hydrostatic stress, deviatoric stress), which are mesh-dependent, the SED averaged over a control volume is insensitive to the mesh refinement. As widely documented in [43,44] dealing with sharp V-notches, refined meshes are not necessary, because the mean value of the SED on the control volume can be directly determined *via* the nodal displacements, without involving their derivatives. As soon as the average SED is known, the notch stress intensity factors (NSIFs) quantifying the asymptotic stress distributions can be calculated *a posteriori* on the basis of very simple expressions linking the local SED and the relevant NSIFs. This holds true also for the stress concentration factors (SCFs), at least when the local stress distributions ahead of the blunt notch are available for the plane problem. The extension of the SED method to three-dimensional cases is also possible as well as its extension to notched geometries exhibiting small scale yielding [45].

Dealing with the SED approach, the main properties of the material are the ultimate tensile strength $\sigma_t = 46$ MPa and the fracture toughness $K_{Ic} = 1.06\ \mathrm{MPa}\sqrt{\mathrm{m}}$. Using Eq. (5), the critical value of SED for the tested material is found to be $W_c = 0.13\ \mathrm{MJ/m^3}$, whereas the radius of the control volume is $R_c \cong 0.17$ mm, considering realistic plane strain conditions.

In the absence of specific data from cracked components, the parameter K_{Ic} can be estimated considering the results from the three specimens with the minimum available radius, $\rho = 0.25$ mm, and $\beta = 0°$. In parallel, the tensile strength has been evaluated using the experimental data from the samples with $\rho = 4$ mm and $\beta = 0°$, according to some indications drawn by Seweryn [3].

Table 4 summarises the values of SED as directly evaluated by means of the numerical models. The table also gives the maximum value of the principal stress (σ_{max}) and the SED value as obtained from the FE models of the graphite specimens by applying to the model the mean value of the critical loads. It is interesting to observe that the maximum principal stress along the notch edge is much greater (about two times) than the ultimate tensile stress of the material justifying the SED approach based on a control volume.

The stress component $\sigma_{\theta\theta}$ is plotted in Fig. 8 versus the normalised distance ξ/ρ. The inclined path is perpendicular to the notch edge and starts from the point on the notch profile where the stress component $\sigma_{\theta\theta}$ is maximum. The finite element results are compared with the mode I theoretical solution given by Creager and Paris for the 'blunt crack' case [46]. The agreement is satisfactory also under prevalent mode II, independent of the notch radius. In parallel, the shear stress component has been verified to be close to zero, as it happens along the notch bisector under pure mode I loading conditions. This observation leads to the conclusion that under mixed mode loading the line normal to the notch edge and starting from the point of maximum principal stress behaves as a virtual bisector line under pure mode I, confirming the applicability of the equivalent local mode I concept.

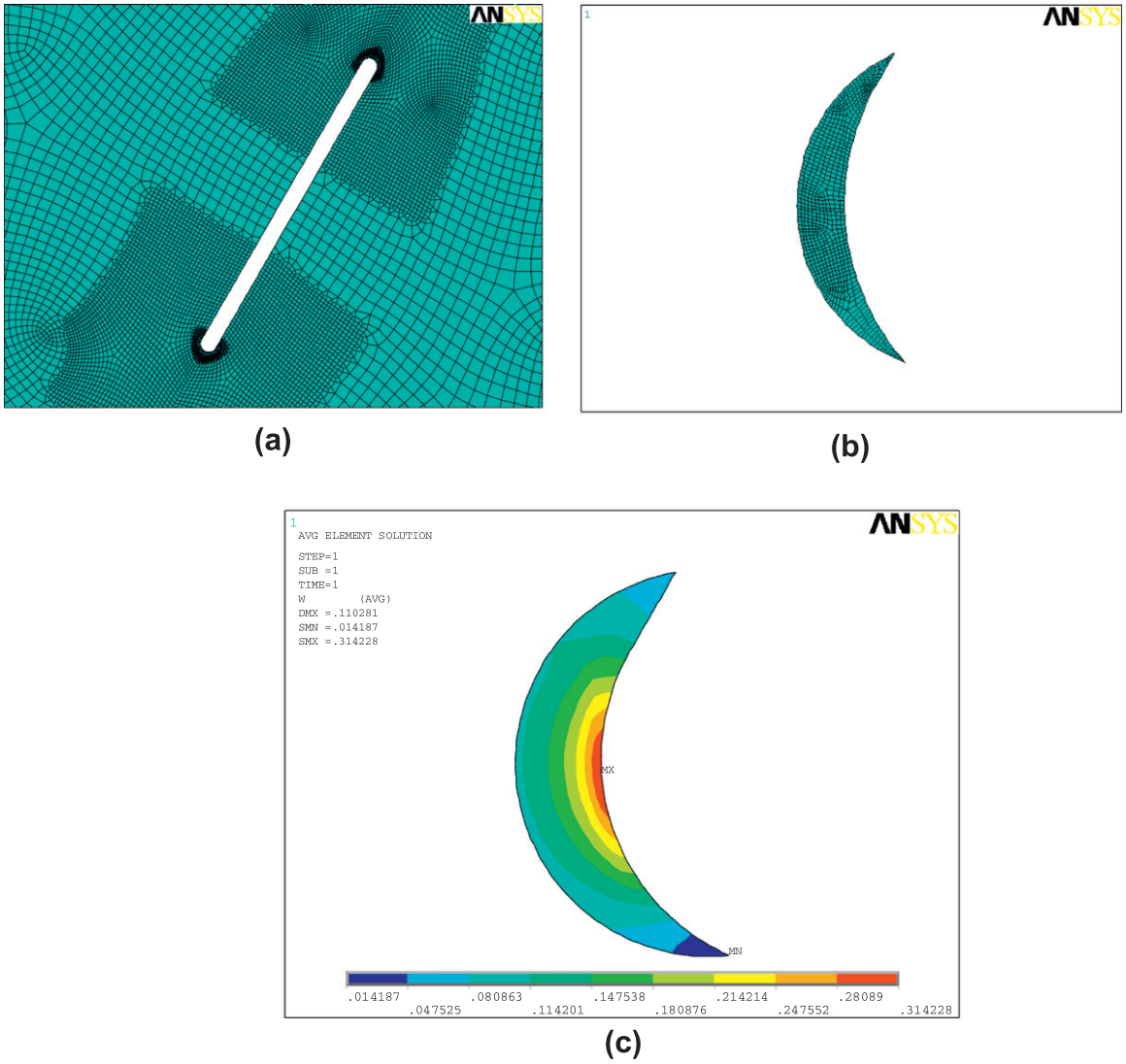

Fig. 6. Typical mesh used to evaluate the SED (a), control volume (b) and SED contour lines (c).

4. Results and discussion

As underlined in Refs. [29–33] dealing with mixed mode loading, particularly for notches with a non-negligible root radius, providing a suitable fracture criterion is more complex than under mode I loading because the maximum elastic stress is out of the notch bisector line and its position strongly varies on the notch edge as a function of mode I to mode II stress distributions. The problem is solved here by applying the SED criterion to rounded-tip U-notched domains, with the aim to estimate the fracture load of notched graphite components.

As underlined before, the purpose of this research is twofold: to provide a new set of experimental data from brittle fractures under mixed mode of an isostatic graphite with a low mean grain size, and to document the applicability of the local SED method in the presence of U-notches, by rigidly rotating the crescent shape volume defined under mode I loading.

The experimental results are summarised in Table 2 whereas a comparison between experimental data and theoretical results is documented in Table 5. The average value of the measured critical loads are compared with the values computed by assuming a constant critical strain energy density over the control volume ($W_c = 0.13$ MJ/m^3). A good agreement can be observed from the table.

Figs. 9–12 plot the experimental results and the theoretical predictions based on the SED approach as a function of the notch root radius for each value of the tilt angle, β.

The relative deviation between experimental and predicted values ranges from −7% to +7%, with an exception (+12%) in the case $\rho = 4$ mm and $\beta = 60°$. However it is important to note that for all the cases taken into account the scatter between theoretical and experimental values is very narrow.

Table 6 summarises the average values of the measured initiation crack angle φ compared with the values obtained from Finite Element analyses. In the numerical analyses the angles where the principal stress (and then the strain energy density) reaches its maximum value along the notch edge has been considered. It is worth nothing from the table that the relative deviation between experimental and predicted results is higher with respect to the case of critical loads as well as the intrinsic scatter of the experimental results (see Figs. 13–15).

As discussed in Refs. [47,48], the finite element technique can be used to calculate the strain energy density (SED) contours and the SED can be used not only to estimate the fracture initiation

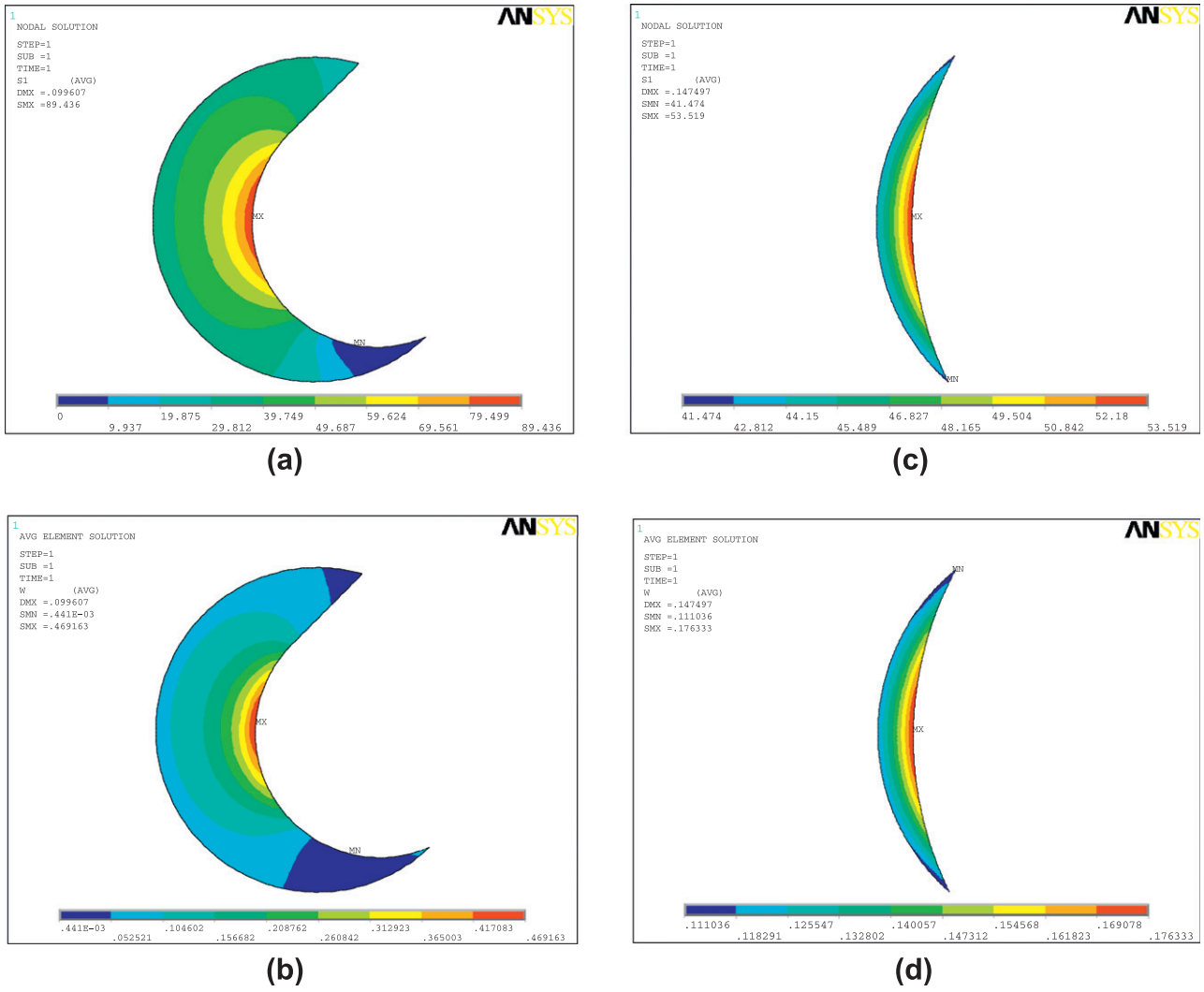

Fig. 7. Contour lines of the maximum principal stress and of the SED in the case $\beta = 45°$ with $\rho = 0.25$ mm (a and b) and $\rho = 2$ mm (c and d).

Table 4
Numerical values of principal stresses and strain energy density.

β (°)	ρ (mm)	φ (°) FEM	σ_{max} (MPa) FEM			$\overline{W}$ (MJ/m^3) FEM			$\langle\overline{W}\rangle$ (MJ/m^3) FEM
0	0.25	0	86.94	99.47	94.14	0.1306	0.1709	0.1531	0.1515
	0.5	0	71.33	69.81	68.81	0.149	0.1428	0.1387	0.1435
	1	0	51.49	59.47	55.76	0.1081	0.1442	0.1267	0.1263
	2	0	45.26	50.87	48.40	0.1009	0.1275	0.1154	0.1146
	4	0	48.08	43.49	46.70	0.1264	0.1034	0.1192	0.1163
30	0.25	34.44	87.95	88.61	90.93	0.135	0.137	0.1443	0.1387
	0.5	32.22	68.37	71.09	70.25	0.1378	0.149	0.1455	0.1441
	1	31.11	56.51	57.37	58.08	0.1315	0.1355	0.1389	0.1353
	2	30.90	53.30	53.83	53.03	0.1408	0.1436	0.1394	0.1412
	4	30.00	47.63	50.58	48.98	0.1243	0.1402	0.1315	0.132
45	0.25	47.78	86.36	88.74	89.30	0.1291	0.1363	0.1381	0.1345
	0.5	46.67	70.59	68.32	70.84	0.1445	0.1353	0.1455	0.1418
	1	46.67	58.15	59.24	57.81	0.1388	0.1441	0.1372	0.1401
	2	46.11	51.19	53.23	53.52	0.1302	0.1408	0.1423	0.1377
	4	45.28	53.24	51.41	51.02	0.1557	0.1452	0.143	0.1479
60	0.25	56.67	87.32	83.28	85.38	0.13	0.1182	0.1243	0.1242
	0.5	57.78	73.28	72.55	74.74	0.1513	0.1484	0.1574	0.1524
	1	58.89	57.97	59.59	59.37	0.1343	0.1419	0.1409	0.139
	2	58.89	53.86	52.41	53.66	0.1428	0.1352	0.1417	0.1399
	4	59.45	56.61	53.85	54.68	0.1757	0.159	0.1639	0.1662

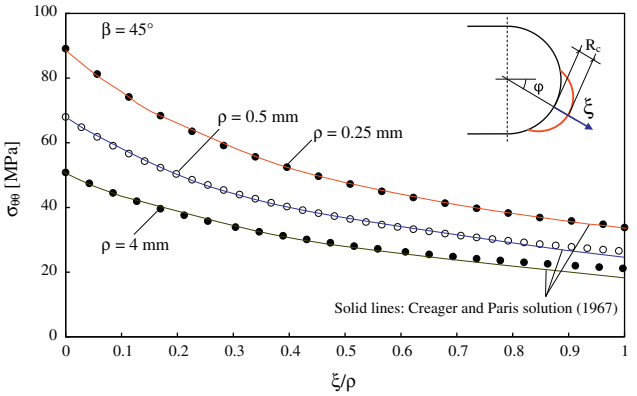

Fig. 8. Stress distribution along the line of maximum tangential stress out of the notch bisector line; $\beta = 45°$ and applied load equal to average value of the experimental loads, $\langle F \rangle$.

Table 5
Comparison between experimental and theoretical critical loads.

β (°)	ρ (mm)	$\langle F_{EXP} \rangle$ (N) Exp.	$\langle F_{th} \rangle$ (N) Theor.	F_{EXP}/F_{th}
0	0.25	4426	4128	1.072
	0.5	4505	4313	1.045
	1	4815	4919	0.979
	2	5516	5914	0.933
	4	6789	7223	0.940
30	0.25	4034	3927	1.027
	0.5	4349	4154	1.047
	1	4824	4755	1.015
	2	5916	5707	1.037
	4	6886	6874	1.002
45	0.25	3927	3882	1.012
	0.5	4261	4103	1.038
	1	4777	4628	1.032
	2	5603	5474	1.024
	4	6862	6469	1.061
60	0.25	3942	4056	0.972
	0.5	4551	4227	1.077
	1	4779	4646	1.028
	2	5455	5288	1.032
	4	6749	6004	1.124

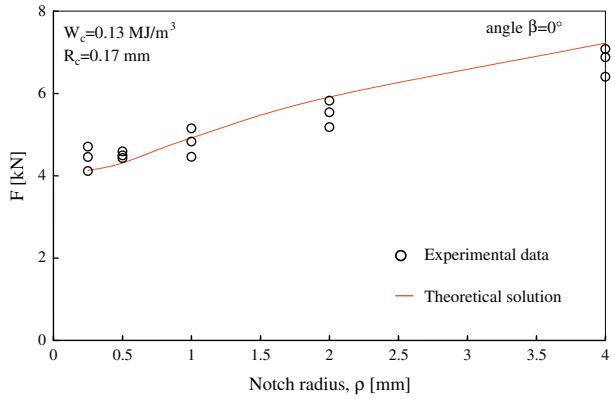

Fig. 9. Comparison between experimental and predicted values of the critical load for different notch radii and tilt angle of the notch $\beta = 0°$.

but also the crack propagation inside the material. The predicted trajectory of the crack during stable and unstable propagation can be assumed to coincide with the minimum of the strain energy density function according to the SED criterion [18]. This simple

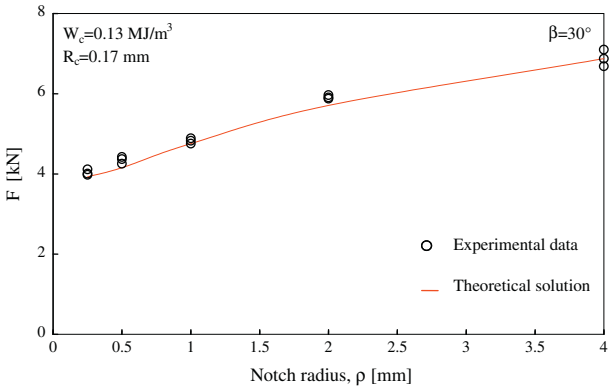

Fig. 10. Comparison between experimental and predicted values of the critical load for different notch radii and tilt angle of the notch $\beta = 30°$.

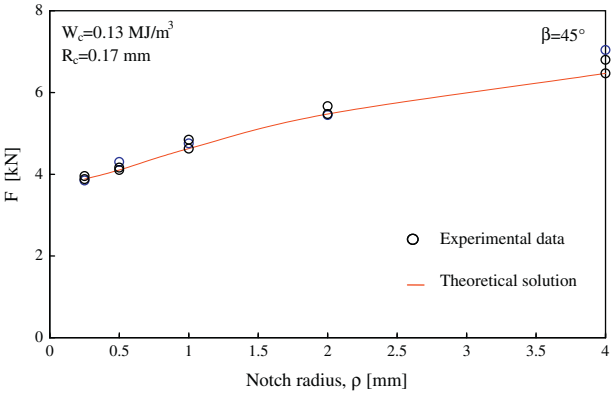

Fig. 11. Comparison between experimental and predicted values of the critical load for different notch radii and tilt angle of the notch $\beta = 45°$.

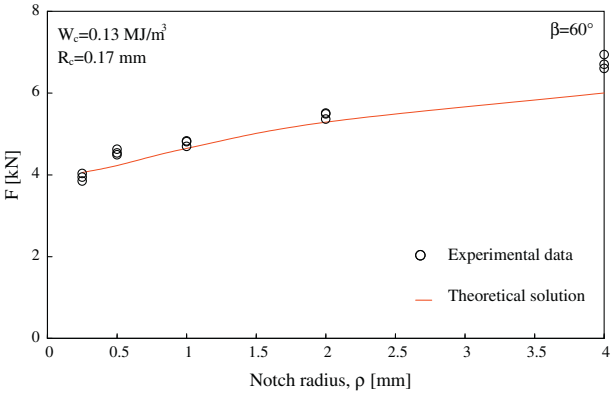

Fig. 12. Comparison between experimental and predicted values of the critical load for different notch radii and tilt angle of the notch $\beta = 60°$.

method has been found to offer a reliable prediction of the crack path stability for two as well as three-dimensional problems with complex geometry structures and arbitrary loadings. In Ref. [48] both Three Point Bending (TPB) and Double Cantilever Beam (DCB) specimens have been analysed showing a good agreement with a large number of experimental results taken from the literature.

The scatter of the critical loads to failure presented here is in good agreement with that documented in Refs. [49,50] where a synthesis based on more than one thousand experimental data

Table 6
Comparison between experimental and numerical initial crack angles.

β (°)	ρ (mm)	$\langle\varphi\rangle$ (°) FEM	$\langle\varphi_{EXP}\rangle$ (°) Exp.	$\Delta\varphi$ (%)
0	0.25	0	0	0
	0.5	0	0	0
	1	0	0	0
	2	0	0	0
	4	0	0	0
30	0.25	34.44	30.82	10.5
	0.5	32.22	35.50	−10.2
	1	31.11	30.11	3.2
	2	30.9	28.30	8.4
	4	30	30.49	−1.6
45	0.25	47.78	42.45	11.2
	0.5	46.67	46.39	0.6
	1	46.67	49.29	−5.6
	2	46.11	44.15	4.2
	4	45.28	47.84	−5.7
60	0.25	56.67	58.23	−2.8
	0.5	57.78	55.84	3.4
	1	58.89	60.74	−3.1
	2	58.89	56.57	3.9
	4	59.45	58.12	2.2

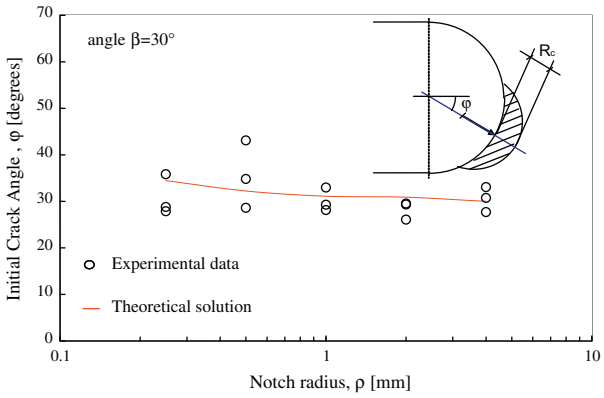

Fig. 13. Comparison between experimental and numerical values of the initial crack angle for different notch radii and tilt angle of the notch $\beta = 30°$.

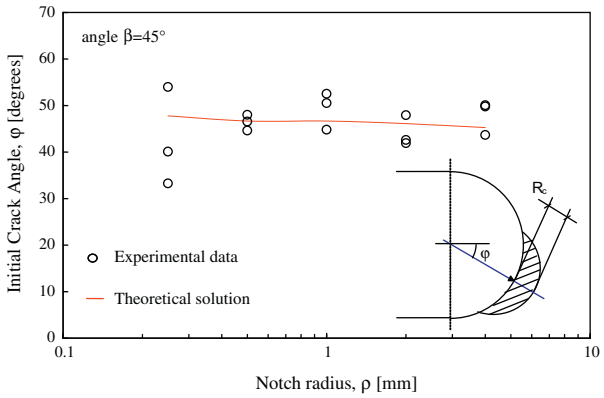

Fig. 14. Comparison between experimental and numerical values of the initial crack angle for different notch radii and tilt angle of the notch $\beta = 45°$.

taken from the recent literature were summarised in terms of SED. Those data came from tests on U- and V-notched specimens made of very different materials and subjected to mode I and mode II loading.

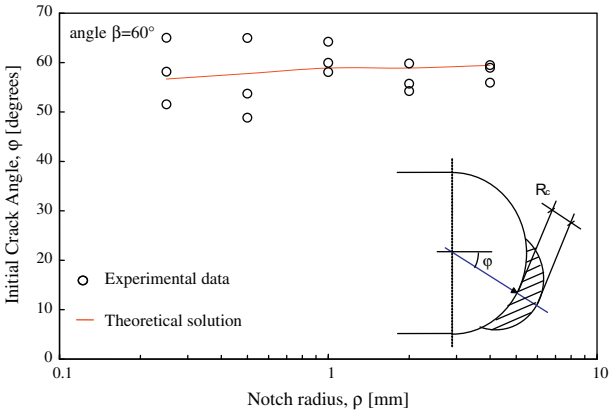

Fig. 15. Comparison between experimental and numerical values of the initial crack angle for different notch radii and tilt angle of the notch $\beta = 60°$.

The proposed scatter band was plotted by using, as a synthesis parameter, the square root value of the local energy averaged over the control volume, normalised with respect to the critical energy of the material. This parameter was plotted as a function of the notch radius to control radius ratio, ρ/R_c. The data were characterised by a high variability of the ratio ρ/R_c, which ranged from about 0 to 1000. The fracture toughness K_{Ic} and the ultimate fracture stress ranged from 0.15 to 55 MPa$\sqrt{m}$ and from 2.5 to 1200 MPa, respectively. The non-negligible influence of the Poisson's ratio was also underlined. The materials were characterised by a critical radius ranging from 0.4 to 500 μm. Data from graphite specimens were not included in that synthesis. The new analyses represent an extension of the previous database, with values of R_c close to the minimum and the maximum values of the previously considered range.

A synthesis in terms of the square root value of the local energy averaged over the control volume, normalised with respect to the critical energy of the material, as a function of the notch tip radius is shown in Fig. 16 while the mean values detailed are listed in Table 7. Together with the new data, the normalised scatterband includes also previous results from V-shaped notches [36]. The plotted parameter is proportional to the fracture load. Fig. 16 makes it evident that the scatter of the data is quite limited, and independent both of the loading mode and the notch root radius. All the values fall well inside a band where the square root of the normalised SED ranges from 0.80 to 1.20. The synthesis confirms also that the choice of the crescent shape volume surround-

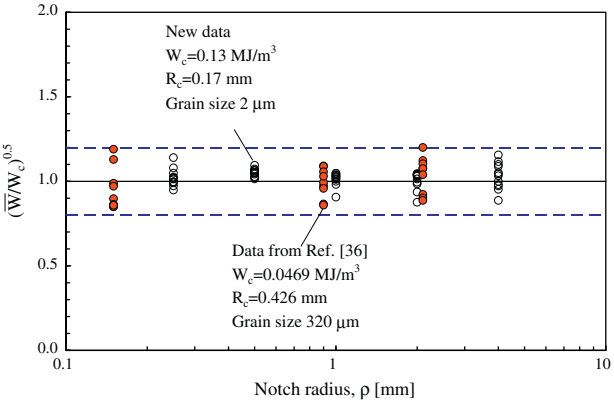

Fig. 16. Scatterband summarising new data and old data taken from Ref. [36] based on an isostatic graphite with an average grain size equal to 320 μm and lower mechanical properties.

Table 7
Comparison between experimental and theoretical critical SED.

β (°)	ρ (mm)	$\langle \overline{W} \rangle$ (MJ/m^3) FEM	W_c (MJ/m^3) Theor.	$(\overline{W}/W_c)^{0.5}$
0	0.25	0.1515	0.1314	1.074
	0.5	0.1435		1.045
	1	0.1263		0.98
	2	0.1146		0.934
	4	0.1163		0.941
30	0.25	0.1387	0.1314	1.027
	0.5	0.1441		1.047
	1	0.1353		1.015
	2	0.1412		1.037
	4	0.132		1.002
45	0.25	0.1345	0.1314	1.012
	0.5	0.1418		1.039
	1	0.1401		1.032
	2	0.1377		1.024
	4	0.1479		1.061
60	0.25	0.1242	0.1314	0.972
	0.5	0.1524		1.077
	1	0.139		1.029
	2	0.1399		1.032
	4	0.1662		1.124

ing the highly stressed region is suitable to characterise the material behaviour under mixed mode loading.

5. Conclusions

Brittle fracture in U-notched isostatic graphite specimens is investigated both experimentally and theoretically under in plane mixed mode loading. Fracture tests are conducted on U-notched specimens subjected to different degrees of mode mixity, which ranges from pure mode I to almost pure mode II.

The *equivalent local mode I* concept is used here in combination with an approach based on the mean value of the strain energy density (SED), which makes the fracture load assessment independent of the loading angle β. The isostatic graphite tested here is characterised by very low values of the grain size (2 μm) and the control volume (R_c = 0.17 mm). This last value is very different from that detected in previous investigations (R_c = 0.43 mm), where the mean grain size of the graphite was more than 300 μm. Different with respect to the previous studies is also the shape of the notches as well as the stronger variability of the notch tip radius, which ranges here from 0.25 mm to 4.0 mm.

The evaluation of the SED over a control volume rigidly rotated with respect to the mode I case is justified by the analysis of the stress field along the inclined path perpendicular to the notch edge and starting from the point of the maximum elastic stress. The stress components along that line have been proven to be very close to the mode I stress distributions along the notch bisector line.

It is shown that the method based on the local SED is suitable for the graphite stressed under mixed mode loading conditions, being the experimental loads to failure always in good agreement with the values estimated by assuming constant the mean value of the SED over the control volume. From the sound agreement between the theoretical and experimental results, it can be straightforward deduced that for the isostatic graphite the critical energy and the radius of the control volume are both material properties, which depend on the grain size. They do not depend on the in-plane mixed mode loading and the notch acuity and then they can be simply evaluated in pure mode I loading. The synthesis confirms also the choice of a crescent shape volume which seems to be suitable to characterise the material behaviour under different mode mixities.

The experimental angles corresponding to the point of crack initiation are compared with the values obtained from the FE analyses on the basis of maximum values of the principal stress and the strain energy density along the notch edge. The relative deviation is quite limited, but greater than that exhibited from the critical loads to failure.

Future work should be planned to show whether, varying the materials, the constancy of the control radius under mode I and mode II loading remains a realistic assumption also in the presence of small scale yielding conditions. Another intriguing topic will be the extension of the SED approach to the cases of pure compression or combined compression and shear, which should require an update of the control radius R_c, due to the increase the critical strain energy density W_c with respect to the uniaxial tension case.

References

[1] Knésl Z. A criterion of V-notch stability. Int J Fract 1991;48:R79–83.
[2] Nui LS, Chehimi C, Pluvinage G. Stress field near a large blunted tip V-notch and application of the concept of the critical notch stress intensity factor (NSIF) to the fracture toughness of very brittle materials. Eng Fract Mech 1994;49:325–35.
[3] Seweryn A. Brittle fracture criterion for structures with sharp notches. Eng Fract Mech 1994;47:673–81.
[4] Strandberg M. Fracture at V-notches with contained plasticity. Eng Fract Mech 2002;69:403–15.
[5] Gogotsi GA. Fracture toughness of ceramics and ceramic composites. Ceram Int 2003;7:777–884.
[6] Gómez FJ, Elices M, Valiente A. Cracking in PMMA containing U-shaped notches. Fatigue Fract Eng Mater Struct 2000;23:795–803.
[7] Gómez FJ, Elices M. A fracture criterion for sharp V-notched samples. Int J Fract 2003;123:163–75.
[8] Ghasemnejad H, Aboutorabi A. Cohesive zone modeling (CZM) in prediction of delamination failure in laminated composite structures. J Mat Sci Eng 2011;5:61–4.
[9] Lazzarin P, Zambardi R. A finite-volume-energy based approach to predict the static and fatigue behaviour of components with sharp V-shaped notches. Int J Fract 2001;112:275–98.
[10] Lazzarin P, Lassen T, Livieri P. A notch stress intensity approach applied to fatigue life predictions of welded joints with different local toe geometry. Fatigue Fract Eng Mater Struct 2003;26:49–58.
[11] Yosibash Z, Bussiba A, Gilad I. Failure criteria for brittle elastic materials. Int J Fract 2004;125:307–33.
[12] Matvienko YG, Morozov EM. Calculation of the energy *J*-integral for bodies with notches and cracks. Int J Fract 2004;125:249–61.
[13] Barati E, Alizadeh Y, Aghazadeh J, Berto F. Some new practical equations for rapid calculation of *J*-integral in plates weakened by U-notches under bending. Mater Des 2010;31:2964–71.
[14] Barati E, Aghazadeh Mohandesi J, Alizadeh Y. The effect of notch depth on *J*-integral and critical fracture load in plates made of functionally graded aluminum–silicone carbide composite with U-notches under bending. Mater Des 2010;31:4686–92.
[15] Ayatollahi MR, Torabi AR. Brittle fracture in rounded-tip V-shaped notches. Mater Des 2010;31:60–7.
[16] Gomez FJ, Guinea GV, Elices M. Failure criteria for linear elastic materials with U-notches. Int J Fract 2006;141:99–113.
[17] Erdogan F, Sih CG. On the crack extension in plates under plane loading and transverse shear. J Basic Eng 1963;85:528–34.
[18] Sih GC. Strain-energy-density factor applied to mixed mode crack problems. Int J Fract 1974;10:305–21.
[19] Papadopoulos GA, Paniridis PI. Crack initiation from blunt notches under biaxial loading. Eng Fract Mech 1988;31:65–78.
[20] Seweryn A, Lucaszewicz A. Verification of brittle fracture criteria for elements with V-shaped notches. Eng Fract Mech 2002;69:1487–510.
[21] Yosibash Z, Priel E, Leguillon D. A failure criterion for brittle elastic materials under mixed-mode loading. Int J Fract 2006;141:291–312.
[22] Priel E, Yosibash Z, Leguillon D. Failure initiation of a blunt V-notch tip under mixed mode loading. Int J Fract 2008;149:143–73.
[23] Chen DH, Ozaki S. Investigation of failure criteria for a sharp notch. Int J Fract 2008;152:63–74.
[24] Ayatollahi MR, Torabi AR. Determination of mode II fracture toughness for U shaped notches using Brazilian disc specimen. Int J Solids Struct 2010;47:454–65.
[25] Ayatollahi MR, Torabi AR. Investigation of mixed mode brittle fracture in rounded-tip V-notched components. Eng Fract Mech 2010;77:3087–104.
[26] Lazzarin P, Berto F. Some expressions for the strain energy in a finite volume surrounding the root of blunt V-notches. Int J Fract 2005;135:161–85.

[27] Berto F, Croccolo D, Cuppini R. Fatigue strength of a fork-pin equivalent coupling in terms of the local strain energy density. Mater Des 2008;29:1780–92.
[28] Berto F, Barati E. Fracture assessment of U-notches under three point bending by means of local energy density. Mater Des 2011;32:822–30.
[29] Gomez FJ, Elices M, Berto F, Lazzarin P. Local strain energy to assess the static failure of U-notches in plates under mixed mode loading. Int J Fract 2007;145:29–45.
[30] Berto F, Lazzarin P, Gómez FJ, Elices M. Fracture assessment of U-notches under mixed mode loading: two procedures based on the equivalent local mode I concept. Int J Fract 2007;148:415–33.
[31] Gómez FJ, Elices M, Berto F, Lazzarin P. A generalized notch stress intensity factor for U-notched components loaded under mixed mode. Eng Fract Mech 2008;75:4819–33.
[32] Gómez FJ, Elices M, Berto F, Lazzarin P. Fracture of V-notched specimens under mixed mode (I + II) loading in brittle materials. Int J Fract 2009;159:121–35.
[33] Gómez FJ, Elices M, Berto F, Lazzarin P. Fracture of U-notched specimens under mixed mode experimental results and numerical predictions. Eng Fract Mech 2009;76:236–49.
[34] Berto F, Ayatollahi MR. Fracture assessment of Brazilian disc specimens weakened by blunt V-notches under mixed mode loading by means of local energy. Mater Des 2011;32:2858–69.
[35] Ayatollahi MR, Torabi AR. Tensile fracture in notched polycrystalline graphite specimens. Carbon 2010;48:2255–65.
[36] Ayatollahi MR, Berto F, Lazzarin P. Mixed mode brittle fracture of sharp and blunt V-notches in polycrystalline graphite. Carbon 2011;49:2465–74.
[37] Berto F, Lazzarin P, Ayatollahi MR. Brittle fracture of sharp and blunt V-notches in isostatic graphite under torsion loading. Carbon 2012;50:1942–52.
[38] Mostafavi M, Marrow TJ. Quantitative in situ study of short crack propagation in polygranular graphite by digital image correlation. Fatigue Fract Eng Mater Struct 2012. http://dx.doi.org/10.1111/j.1460-2695.2012.01648.x.
[39] Lomakin EV, Zobnin AI, Berezin AV. Finding the fracture toughness characteristics of graphite materials in plane strain. Strength Mater 1975;7:484–7.
[40] Yamauchi Y, Nakano M, Kishida K, Okabe T. Measurement of mixed-mode fracture toughness for brittle materials using edge-notched half-disk specimen. Zairyo/J Soc Mater Sci Jpn 2001;50:224–9.
[41] Lazzarin P, Filippi S. A generalised stress intensity factor to be applied to rounded V-shaped notches. Int J Solids Struct 2006;43:2461–78.
[42] Lazzarin P, Zappalorto M, Berto F. Generalised stress intensity factors for rounded notches in plates under in-plane shear loading. Int J Fract 2011;170:123–44.
[43] Lazzarin P, Berto F, Gómez FJ, Zappalorto M. Some advantages derived from the use of the strain energy density over a control volume in fatigue strength assessments of welded joints. Int J Fatigue 2008;30:1345–57.
[44] Lazzarin P, Berto F, Zappalorto M. Rapid calculations of notch stress intensity factors based on averaged strain energy density from coarse meshes: theoretical bases and applications. Int J Fatigue 2010;32:1559–67.
[45] Lazzarin P, Berto F. Control volumes and strain energy density under small and large scale yielding due to tensile and torsion loading. Fatigue Fract Eng Mater Struct 2008;31:95–107.
[46] Creager M, Paris PC. Elastic field equations for blunt cracks with reference to stress corrosion cracking. Int J Fract Mech 1967;3:247–52.
[47] Zheng M, Zhou G, Zacharopoulos DA, Kuna M. Crack initiation behavior in StE690 Steel characterized by strain energy density criterion. Theor Appl Fract Mech 2001;36:141–5.
[48] Zacharopoulos DA. Stability analysis of crack path using the strain energy density. Theor Appl Fract Mech 2004;41:327–37.
[49] Lazzarin P, Berto F, Elices M, Gómez J. Brittle failures from U- and V-notches in mode I and mixed, I + II, mode. A synthesis based on the strain energy density averaged on finite size volumes. Fatigue Fract Eng Mater Struct 2009;32:671–84.
[50] Berto F, Lazzarin P. A review of the volume-based strain energy density approach applied to V-notches and welded structures. Theor Appl Fract Mech 2009;52:183–94.